


# SCIENTIFIC REPORTS



OPEN

## Eosinophils support adipocyte maturation and promote glucose tolerance in obesity

Eun-Hui Lee<sup>1</sup>, Michal Itan<sup>2</sup>, Jinsun Jang<sup>1,3</sup>, Hyeon-Jung Gu<sup>1,8</sup>, Perri Rozenberg<sup>2</sup>, Melissa K. Mingler<sup>4</sup>, Ting Wen<sup>4</sup>, Jiyoung Yoon<sup>1</sup>, Shi-Young Park<sup>5,6</sup>, Joo Young Roh<sup>3</sup>, Cheol Soo Choi<sup>5,6</sup>, Woo-Jae Park<sup>7,8</sup>, Ariel Munitz<sup>2</sup> & YunJae Jung<sup>1,8</sup> 

Accumulating data have indicated a fundamental role of eosinophils in regulating adipose tissue homeostasis. Here, we performed whole-genome RNA sequencing of the small intestinal tract, which suggested the presence of impaired lipid metabolism in eosinophil-deficient  $\Delta$ dblGATA mice.  $\Delta$ dblGATA mice fed a high-fat diet (HFD) showed reduced body fat mass, impaired enlargement of adipocytes, decreased expression of adipogenic genes, and developed glucose intolerance. HFD induced accumulation of eosinophils in the perigonadal white adipose tissue. Concordantly, adipocyte-differentiated 3T3-L1 cells promoted the migration of eosinophils through the expression of CCL11 (eotaxin-1) and likely promoted their survival through the expression of interleukin (IL)-3, IL-5, and granulocyte-macrophage colony-stimulating factor. HFD-fed  $\Delta$ dblGATA mice showed increased infiltration of macrophages, CD4<sup>+</sup> T-cells, and B-cells, increased expression of interferon- $\gamma$ , and decreased expression of IL-4 and IL-13 in white adipose tissue. Interferon- $\gamma$  treatment significantly decreased lipid deposition in adipocyte-differentiated 3T3-L1 cells, while IL-4 treatment promoted lipid accumulation. Notably, HFD-fed  $\Delta$ dblGATA mice showed increased lipid storage in the liver as compared with wild-type mice. We propose that obesity promotes the infiltration of eosinophils into adipose tissue that subsequently contribute to the metabolic homeostasis by promoting adipocyte maturation.

Eosinophils have been considered as destructive cells involved in T helper cell type (Th) 2 immune responses in parasitic infections or allergic diseases<sup>1</sup>. However, accumulating evidence has indicated additional roles for eosinophils. For example, eosinophils reside in several organs including the gastrointestinal tract<sup>2,3</sup> and adipose tissue and contribute to metabolic homeostasis<sup>4,5</sup>. Adipose tissue eosinophils secrete interleukin (IL)-4 and induce the polarization of white adipose tissue (WAT) macrophages into alternatively-activated macrophages, which support glucose tolerance by regulating local catecholamine stores in the microenvironment through the import of catecholamines produced by nerve cells<sup>4,6,7</sup>. Despite recent advances, the roles of eosinophils in the adipose tissue and their effects on adipocyte function remain incompletely understood.

Obesity and its associated metabolic disorders are serious health problems worldwide<sup>8</sup>. However, obesity is not necessarily an adverse metabolic condition when the excess fat is stored in adipose tissue that responds to insulin<sup>9</sup>. Adipose tissue regulates energy homeostasis through the storage of excess calories and the secretion of adipocyte-derived secretory proteins such as leptin, adiponectin, and resistin<sup>10,11</sup>. However, excessive caloric

<sup>1</sup>Department of Microbiology, School of Medicine, Gachon University, Incheon, 21999, Korea. <sup>2</sup>Department of Clinical Microbiology and Immunology, The Sackler School of Medicine, Tel-Aviv University, Ramat Aviv, 69978, Israel. <sup>3</sup>Department of Dermatology, Gachon Gil Medical Center, School of Medicine, Gachon University, Incheon, 21565, Korea. <sup>4</sup>Division of Allergy and Immunology, Cincinnati Children's Hospital Medical Center, University of Cincinnati College of Medicine, Cincinnati, OH, 45229, USA. <sup>5</sup>Department of Molecular Medicine, Lee Gil Ya Cancer and Diabetes Institute, School of Medicine, Gachon University, Incheon, 21999, Korea. <sup>6</sup>Korea Mouse Metabolic Phenotyping Center, Lee Gil Ya Cancer and Diabetes Institute, School of Medicine, Gachon University, Incheon, 21999, Korea. <sup>7</sup>Department of Biochemistry, School of Medicine, Gachon University, Incheon, 21999, Korea. <sup>8</sup>Gachon Advanced Institute for Health Science & Technology, Gachon University, Incheon, 21999, Korea. Eun-Hui Lee and Michal Itan contributed equally to this work. Correspondence and requests for materials should be addressed to Y.J. (email: [yjjung@gachon.ac.kr](mailto:yjjung@gachon.ac.kr))

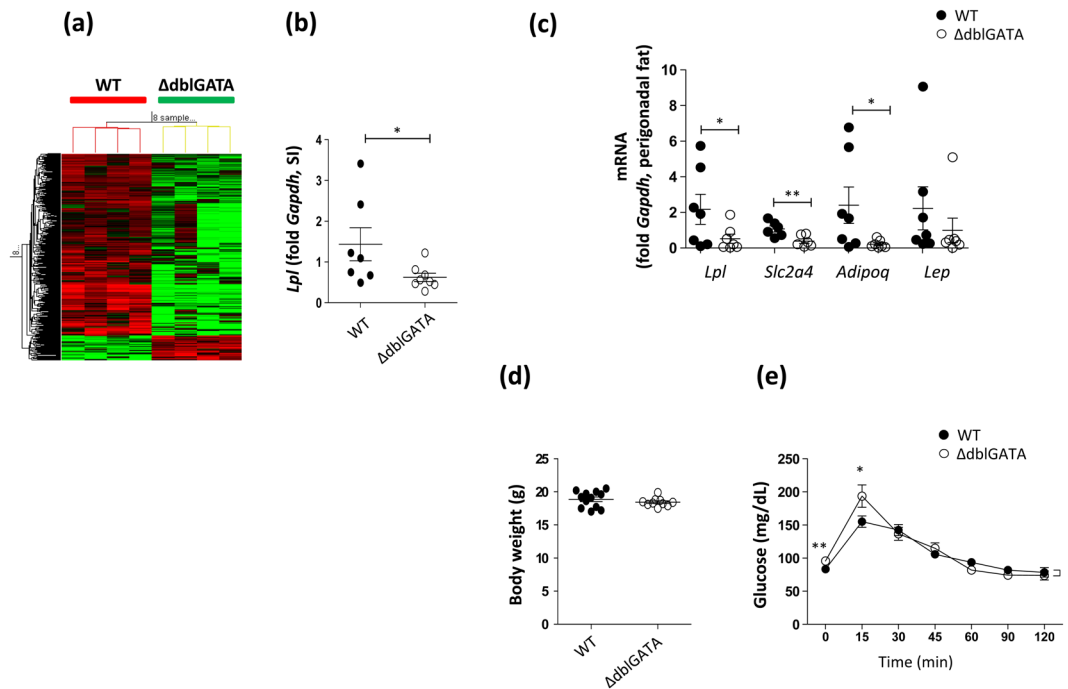


**Figure 1.**  $\Delta$ dblGATA mice showed impaired glucose tolerance and a decreased expression of genes involved in energy metabolism. (a) RNA sequencing data obtained from the small intestine (SI) of 8–10-week-old wild-type (WT) and  $\Delta$ dblGATA mice. The expression of 379 downregulated and 52 upregulated genes was observed in  $\Delta$ dblGATA mice with a fragments per kilobase of exon per million fragments mapped value  $>0.1$  in at least 1 out of 8 analysed samples. Red indicates a high expression and green indicates a low expression. (b) Real-time PCR analysis of *Lpl* in the SI. \**p* < 0.05 (Student's *t*-test). (c) mRNA expression levels of adipogenic and adipokine genes in the perigonadal fat of 8–10-week-old male mice fed with a chow diet. \**p* < 0.05, \*\**p* < 0.01 (Student's *t*-test for *Lpl*, *Slc2a4*, and *Adipoq*, Mann-Whitney test for *Lep*). (d) Body weight of 8–10-week-old male mice fed with a chow diet. (e) Glucose tolerance test of 8–10-week-old male mice fasted for 16 h (*n* = 10–12 mice/group). \**p* < 0.05, \*\**p* < 0.01 (Student's *t*-test). Graphs show the mean  $\pm$  standard error of the mean.

intake induces the overexpansion of adipocytes, which results in inflammatory responses within adipose tissue<sup>12</sup>. Obesity-related metabolic dysfunctions are associated with an excessive infiltration of immune cells and chronic inflammation in adipose tissue<sup>13,14</sup>.

Here, we used eosinophil-deficient  $\Delta$ dblGATA and wild-type (WT) mice to investigate the roles of eosinophils in obesity, adipose tissue maturation, and associated metabolic responses. We performed whole-genome RNA sequencing of the small intestinal tract, which suggested the presence of a defective lipid metabolism in the absence of eosinophils. Furthermore,  $\Delta$ dblGATA mice fed a high-fat diet (HFD) gained less weight and showed reduced body fat, an impaired enlargement of adipocytes, a decreased expression of adipogenic genes, and a more severe glucose intolerance than the WT group. Thus, we hypothesized that the inability to appropriately expand adipose tissue underlies insulin resistance in  $\Delta$ dblGATA mice. We found that adipocyte-differentiated 3T3-L1 cells promoted the migration of eosinophils through the expression of CC chemokine ligand (CCL) 11 (eotaxin-1) and promoted their survival through the expression of IL-3, IL-5, and granulocyte-macrophage colony-stimulating factor (GM-CSF). Accordingly, the WAT of HFD-fed WT mice showed an increased infiltration of eosinophils with upregulated CCL11. Compared to WT mice,  $\Delta$ dblGATA mice showed significantly increased populations of pro-inflammatory immune cells in their WAT. The WAT of HFD-fed  $\Delta$ dblGATA mice also showed an increased expression of the Th1 cytokine interferon (IFN)- $\gamma$  and a decreased expression of the Th2 cytokines IL-4 and IL-13. The cytokine expression profile of the WAT of  $\Delta$ dblGATA mice negatively correlated with adipocyte maturation as demonstrated by attenuated lipid storage in IFN- $\gamma$ -treated 3T3-L1 cells, which was opposed by IL-4 treatment. Notably, HFD-fed  $\Delta$ dblGATA mice showed increased lipid storage in the liver as compared with WT mice, suggesting that insulin resistance was induced by an excessive accumulation of lipid in non-adipose tissues. Thus, we propose that cross-talk between adipocytes and eosinophils promotes metabolic homeostasis by supporting the infiltration of eosinophils into adipose tissue and maintaining the microenvironment of adipose tissue to favour adipocyte maturation.

## Results

**Eosinophil-deficient mice showed impaired glucose tolerance and a decreased expression of genes involved in energy metabolism.** Under physiological conditions, eosinophils primarily reside in the small intestine, where they account for a substantial fraction (e.g., 20–30%) of the cellular population<sup>2,3</sup>. Therefore, the significant downregulation of genes in the small intestine of  $\Delta$ dblGATA mice may indicate a role

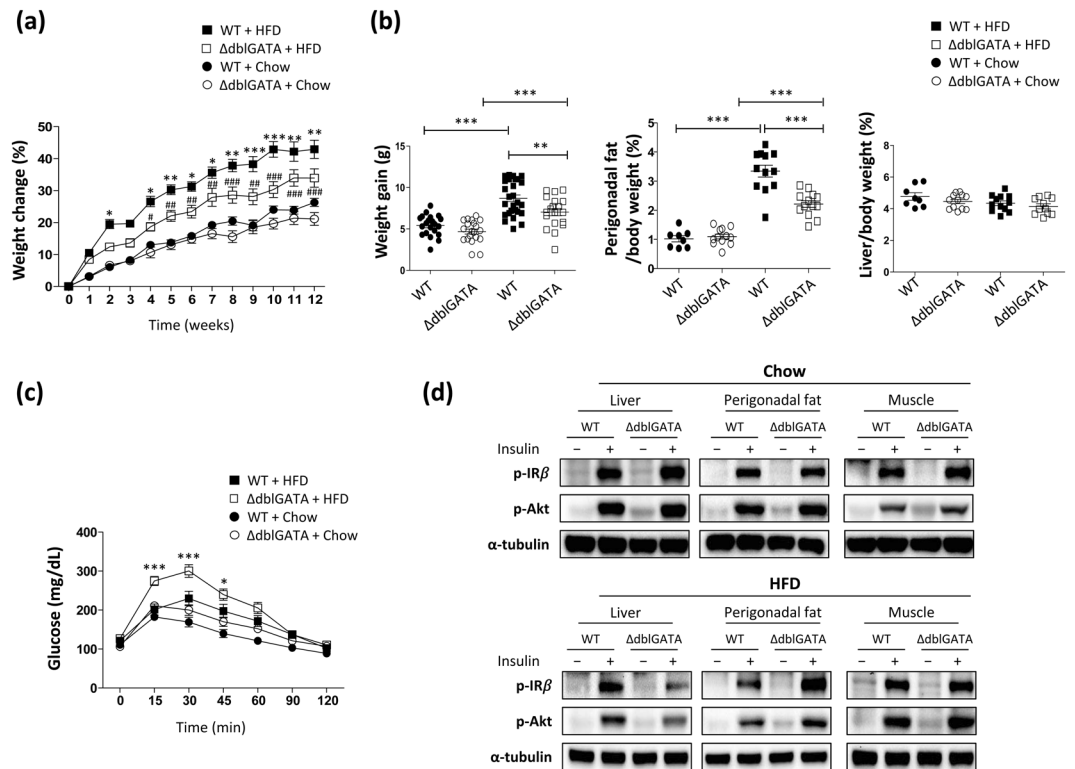


**Figure 2.**  $\Delta$ dblGATA mice gained less weight and body fat and displayed impaired glucose tolerance on a high-fat diet (HFD). Wild-type (WT) and  $\Delta$ dblGATA male mice were fed a HFD or chow diet for 12 weeks. **(a)** Weight change during feeding with a HFD or chow diet ( $n = 20\text{--}27$  mice/group).  $*p < 0.05$ ,  $**p < 0.01$ ,  $***p < 0.001$  (two-way ANOVA), WT + HFD vs.  $\Delta$ dblGATA + HFD.  $\#p < 0.05$ ,  $\#\#p < 0.01$ ,  $\#\#\#p < 0.001$  (two-way ANOVA),  $\Delta$ dblGATA + Chow vs.  $\Delta$ dblGATA + HFD. **(b)** Body weight gain, perigonadal fat/body mass, and liver/body mass on a HFD or chow diet.  $**p < 0.01$ ,  $***p < 0.001$  (one-way ANOVA). **(c)** Glucose tolerance test of the indicated mice fasted for 16 h ( $n = 13\text{--}15$  mice/group).  $*p < 0.05$ ,  $***p < 0.001$  (two-way ANOVA), WT + HFD vs.  $\Delta$ dblGATA + HFD. **(d)** Western blots of insulin-stimulated phosphorylation of insulin receptor (IR) and protein kinase B (Akt) in the liver, perigonadal fat, and skeletal muscle. The data are representative of two independent experiments. Graphs show the mean  $\pm$  standard error of the mean.

for eosinophils in regulating certain biological responses. Through the whole-genome RNA sequencing of the small intestine, we observed 379 downregulated and 52 upregulated genes in the small intestine of  $\Delta$ dblGATA mice (Fig. 1a, Tables S1 and S2) and the expression of the top 10 downregulated genes was validated by real-time PCR (Fig. S1). Of note, genes associated with lipid metabolism, such as *Retnlg*, *Alox15*, and *Drd2*<sup>15–17</sup> were included in the top 10 downregulated genes (Table S1). Additionally, a GO analysis of the downregulated genes and visualization of a functionally grouped network using the ClueGO plugin<sup>18</sup> suggested a defect in lipase activity (Table S3 and Fig. S2) and a significant decrease in the expression of *Lpl* was observed (Fig. 1b). A decreased expression of *Lpl* and other lipogenic genes (*Slc2a4* and *Adipoq*) was also observed in the perigonadal WAT of  $\Delta$ dblGATA mice (Fig. 1c). Although the body weight of 8–10-week-old  $\Delta$ dblGATA mice was not different from that of WT mice (Fig. 1d),  $\Delta$ dblGATA mice showed a significantly higher glucose level at the early time point of GTT (Fig. 1e). Our observations suggested that eosinophils regulate lipid metabolism and energy homeostasis.

**Eosinophil-deficient mice gained less weight and perigonadal fat mass and displayed impaired glucose tolerance on a HFD.** Excess caloric intake induces expansion of fat mass and accelerates development of insulin resistance<sup>10</sup>. To further examine the role of eosinophils in adipose tissue expansion and energy homeostasis, we fed 8–10-week-old male WT and  $\Delta$ dblGATA mice with a HFD for 12 weeks and monitored their body weights weekly. The HFD induced a significant weight gain of  $\Delta$ dblGATA mice compared to chow diet-fed  $\Delta$ dblGATA mice (Fig. 2a). However,  $\Delta$ dblGATA mice showed an approximately 20% lower body weight than WT mice after 12 weeks of a HFD (Fig. 2a,b). Consistent with their lesser weight gain,  $\Delta$ dblGATA mice fed a HFD had significantly less perigonadal fat mass than WT mice (Figs 2b and S3a). Differences in liver mass were not apparent among the analysed groups of mice (Figs 2b and S3a). Although  $\Delta$ dblGATA mice showed less weight gain under a HFD than their WT counterparts, their ability to normalize blood glucose in the GTT was significantly impaired (Fig. 2c). HFD-fed  $\Delta$ dblGATA mice showed significantly higher blood glucose levels until 30 min after insulin administration (ITT, Fig. S3b); however, the slopes of the ITT curves between WT and  $\Delta$ dblGATA appear to overlap and blood insulin levels did not differ between WT and  $\Delta$ dblGATA mice (Fig. S3c). To assess the molecular basis of insulin resistance observed in HFD- $\Delta$ dblGATA mice, we investigated insulin

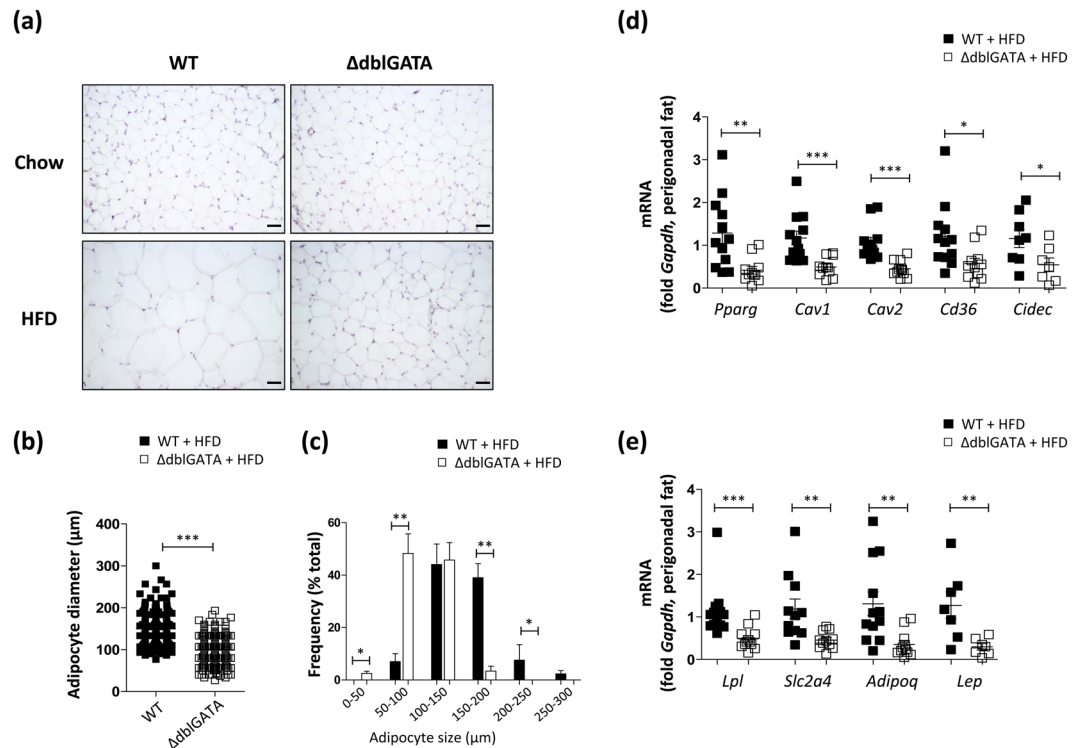


**Figure 3.**  $\Delta$ dblGATA mice showed defective adipocyte enlargement and a decreased expression of genes involved in adipocyte maturation on a high-fat diet (HFD). (a) Haematoxylin and eosin staining of the perigonadal fat of wild-type (WT) and  $\Delta$ dblGATA mice fed a HFD or chow diet. Images are representative of two independent experiments. Original magnification  $\times 20$ . The scale bar represents  $50\mu\text{m}$ . (b,c) Adipocyte size and distribution. (b) Mean adipocyte size and (c) percentile distribution of adipocyte size. Three sections were examined in each group and 2–3 fields were selected from one section.  $*p < 0.05$ ,  $**p < 0.01$ ,  $***p < 0.001$  (Mann-Whitney test). (d and e) mRNA expression levels of (d) adipogenic and (e) adipogenic genes in the perigonadal fat of mice on a HFD.  $*p < 0.05$ ,  $**p < 0.01$ ,  $***p < 0.001$  (Student's *t*-test for *Pparg*, *Cav1*, *Cd36*, *Cidec*, and *Lep*, Mann-Whitney test for *Cav2*, *Lpl*, *Slc2a4*, and *Adipoq*). Graphs show the mean  $\pm$  standard error of the mean.

receptor signalling after infusion of insulin through the portal vein. Insulin receptor (IR) tyrosine phosphorylation and protein kinase B (Akt) phosphorylation were reduced in the livers, but not in WAT or skeletal muscle from HFD-fed  $\Delta$ dblGATA mice compared to in their WT counterparts (Fig. 2d). Phosphorylation of either IR or Akt was comparable between WT and  $\Delta$ dblGATA mice fed a chow diet (Fig. 2d). Taken together, our observations indicate that hepatic insulin resistance was induced in  $\Delta$ dblGATA mice by HFD feeding.

Although  $\Delta$ dblGATA mice fed with HFD showed increased level of serum free fatty acid than WT mice (Fig. S4a), it is unlikely that  $\Delta$ dblGATA mice have defect in energy utilization considering the comparable serum triglyceride and stool fat content of the HFD-fed WT and  $\Delta$ dblGATA mice (Fig. S4a,b). Energy intake and expenditure were also comparable between HFD-fed WT and  $\Delta$ dblGATA mice (Fig. S4c).

### Eosinophil-deficient mice showed an impaired maturation of perigonadal adipocytes on a HFD.

The inability of adipose tissue to expand to accommodate excess calories causes systemic insulin resistance and hyperglycaemia<sup>19</sup>. As we observed an impaired WAT development in HFD-fed  $\Delta$ dblGATA mice, which showed glucose intolerance, we examined whether eosinophils are required for adipocyte maturation in diet-induced obesity. A histological analysis of the perigonadal WAT of HFD-fed  $\Delta$ dblGATA mice illustrated a markedly decreased adipocyte size as compared to WT mice (Fig. 3a). A quantification of the mean diameter of adipocytes in representative histological sections highlighted the significant size difference (Fig. 3b) with a significant increase in small adipocytes in HFD-fed  $\Delta$ dblGATA mice (Fig. 3c). Concordantly, the expression of genes involved in adipocyte differentiation (*Pparg*) and lipid droplet formation (*Cav1*, *Cav2*, *Cd36*, and *Cidec*) was decreased in the WAT of HFD-fed  $\Delta$ dblGATA mice (Fig. 3d). *Pparg* and *Cd36* expression was not decreased in the fat of 8–10 weeks-old  $\Delta$ dblGATA mice fed a chow diet (Fig. S5). The expression of lipogenic markers, including *Adipoq*, which is associated with insulin sensitivity, was also decreased in the WAT of HFD-fed  $\Delta$ dblGATA mice (Fig. 3e).

**Adipocytes support the migration and survival of eosinophils.** Since eosinophils are resident cells in the adipose tissue<sup>20</sup> and  $\Delta$ dblGATA mice showed an impairment of adipocyte maturation, we questioned whether adipocytes support the migration or survival of eosinophils. Eosinophils migrate in a manner dependent on CCL11 and its receptor, CC chemokine receptor (CCR) 3<sup>2,21</sup>. We determined that adipocyte-differentiated

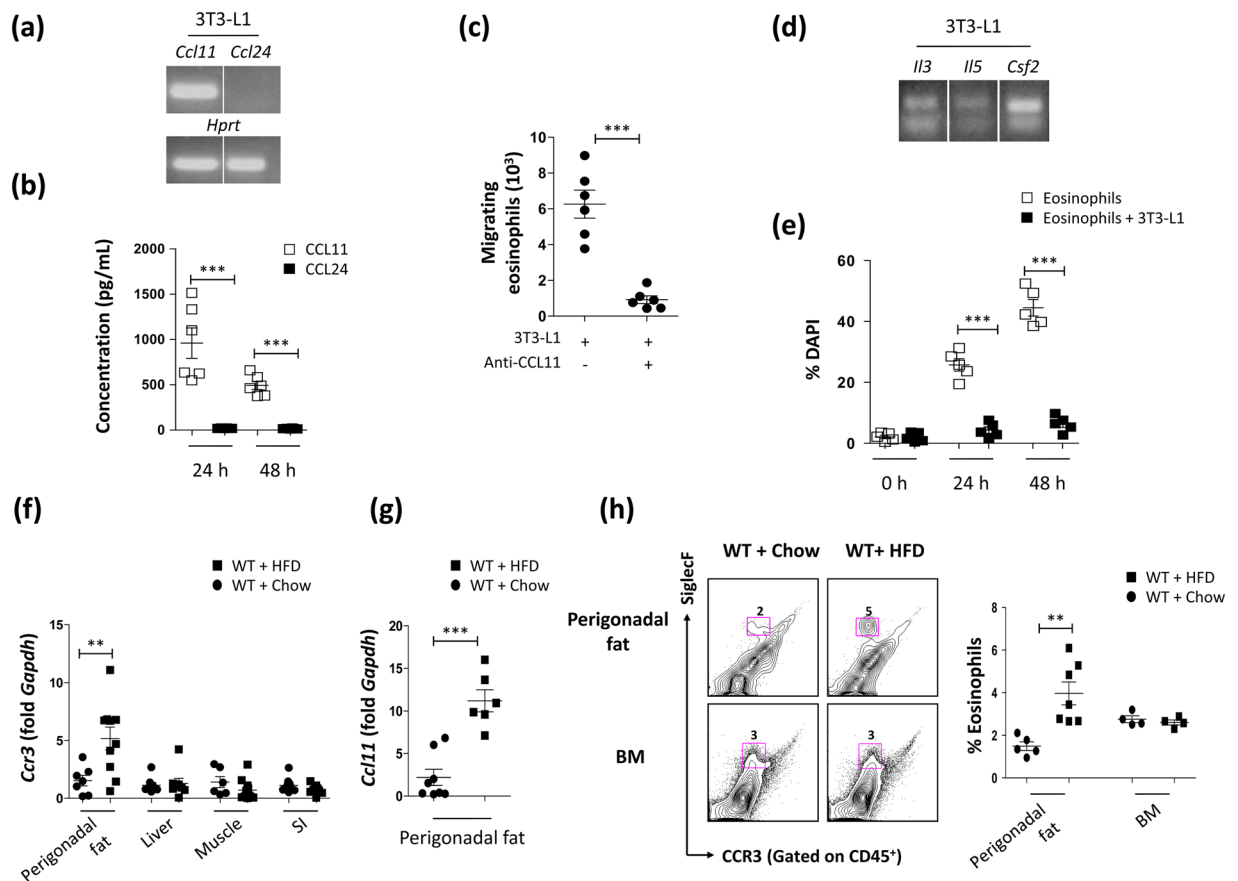


**Figure 4.** Adipocyte-derived molecules that support eosinophil migration and survival account for eosinophil infiltration in the perigonadal adipose tissue of high fat diet (HFD) fed mice. **(a)** mRNA expression of CC chemokine ligand 11 (*Ccl11*) and *Ccl24* in adipocyte-differentiated 3T3-L1 cells. Representative blots from 3 independent experiments. The full-length blots are presented in Fig. S6. \*\*\* $p < 0.001$  (Student's *t*-test) **(b)** Production of CCL11 and CCL24 by cultures of adipocyte-differentiated 3T3-L1 cells. \*\*\* $p < 0.001$  (Student's *t*-test) **(c)** Migration of eosinophils isolated from the peritoneal cavity of CD3-IL-5 transgenic mice toward adipocyte-differentiated 3T3-L1 cells treated with or without anti-mouse CCL11. \*\*\* $p < 0.001$  (Student's *t*-test) **(d)** mRNA expression of interleukin (IL)-3 (*Il3*), IL-5 (*Il5*), and granulocyte-macrophage colony-stimulating factor (*Csf2*) in adipocyte-differentiated 3T3-L1 cells. Representative blots from 3 independent experiments. The full-length blots are presented in Fig. S6. **(e)** Viability of eosinophils isolated from the peritoneal cavity of CD3-IL-5 transgenic mice and co-cultured with or without adipocyte-differentiated 3T3-L1 cells. Non-viable eosinophils were detected by staining with 4',6-diamidino-2-phenylindole dihydrochloride (DAPI). \*\*\* $p < 0.001$  (Student's *t*-test) **(f)** mRNA expression of *Ccr3* in the perigonadal fat, liver, muscle, and small intestine (SI) of wild-type (WT) mice fed a HFD or chow. \*\* $p < 0.01$  (Student's *t*-test for fat, muscle, and SI, Mann-Whitney test for liver). **(g)** mRNA expression of *Ccl11* in the perigonadal fat of WT mice fed a HFD or chow. \*\*\* $p < 0.001$  (Student's *t*-test) **(h)** Flow cytometric analysis of CCR3<sup>+</sup>SiglecF<sup>+</sup> eosinophils in the perigonadal fat and bone marrow (BM) of WT mice fed a HFD or chow. Representative dot plots are shown. \*\* $p < 0.01$  (Student's *t*-test). Graphs show the mean  $\pm$  standard error of the mean.

mouse embryonic fibroblast 3T3-L1 cells expressed *Ccl11* (Figs 4a and S6) and secreted CCL11 (Fig. 4b), which attracted eosinophils, since the application of anti-mouse CCL11 significantly inhibited eosinophil trafficking toward 3T3-L1 cells (Fig. 4c). Additionally, adipocyte-differentiated 3T3-L1 cells expressed cytokines supporting eosinophil survival, such as *Il3*, *Il5*, and *Csf2* (Figs 4d and S6). Accordingly, the viability of eosinophils was markedly increased by co-culture with adipocyte-differentiated 3T3-L1 cells (Fig. 4e). Next, we assessed eosinophil infiltration in the WAT of HFD-fed WT mice and found a significant increase in the expression of *Ccr3* and *Ccl11* in the perigonadal WAT (Fig. 4f,g). An increased frequency and number of eosinophils in the WAT was also supported by a flow cytometry analysis (Figs 4h and S7a). The frequency of eosinophils in the bone marrow was unaffected by the HFD (Fig. 4h). These results imply that eosinophils preferentially migrate to the perigonadal adipose tissue in diet-induced obesity because of the production of molecules that support their migration and survival by adipocytes.

**The perigonadal adipose tissue of eosinophil-deficient mice showed an increased inflammatory response.** Excess calorie intake results in chronic inflammation in adipose tissue involving an infiltration of

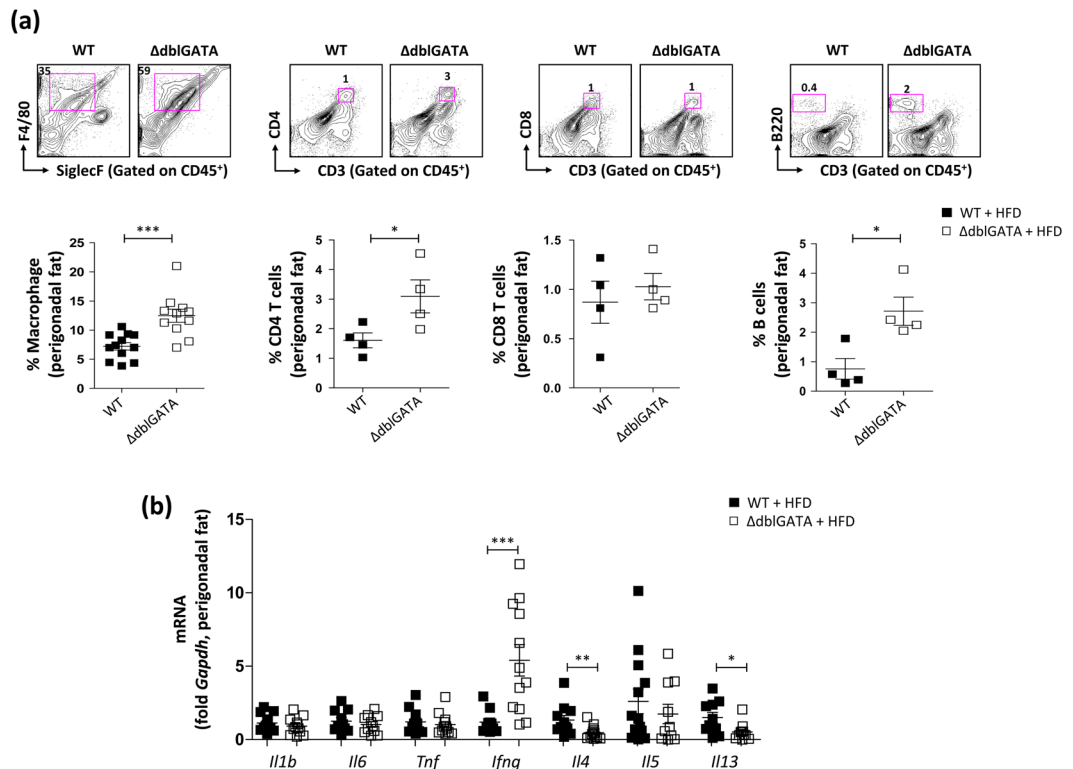


**Figure 5.**  $\Delta$ dblGATA mice showed increased inflammatory responses in the perigonadal adipose tissue on a high fat diet (HFD). **(a)** Flow cytometric analysis of SiglecF<sup>-</sup>F4/80<sup>+</sup> macrophages, CD3<sup>+</sup>CD4<sup>+</sup> T cells, CD3<sup>+</sup>CD8<sup>+</sup> T cells, and CD3<sup>+</sup>B220<sup>+</sup> B cells in the perigonadal fat of wild-type (WT) and  $\Delta$ dblGATA mice on a HFD. Representative dot plots are shown. \* $p < 0.05$ , \*\*\* $p < 0.001$  (Student's *t*-test for macrophage, Mann-Whitney test for CD4 T cells, CD8 T cells, and B cells). **(b)** mRNA expression of innate (*Il1b*, *Il6*, and *Tnf*) and adaptive (*Ifng*, *Il4*, *Il5*, and *Il13*) immune cytokines in the perigonadal fat of mice on a HFD. \* $p < 0.05$ , \*\* $p < 0.01$ , \*\*\* $p < 0.001$  (Student's *t*-test for *Il1b*, *Il6*, *Tnf*, and *Il4*, Mann-Whitney test for *Ifng*, *Il5*, and *Il13*). Graphs show the mean  $\pm$  standard error of the mean.

various immune cells<sup>22–26</sup>. In obesity, the infiltrated immune cells promote the production of pro-inflammatory cytokines that inhibit adipogenesis and insulin signalling<sup>27,28</sup>. The total numbers of cells isolated from the perigonadal WAT of HFD-fed  $\Delta$ dblGATA and WT mice were not significantly different ( $p = 0.1263$ , data not shown). However, significantly increased abundances of macrophages, CD4<sup>+</sup> T cells, and B cells were observed in the perigonadal WAT of HFD-fed  $\Delta$ dblGATA mice (Figs 5a and S7b). Although HFD-fed  $\Delta$ dblGATA mice showed an increased abundance of macrophages in WAT as compared with WT mice, the ratio between the classical (M1) and alternative (M2) immune phenotypes of the macrophages was comparable between  $\Delta$ dblGATA and WT mice (Fig. S8a). This finding was supported by the lack of a significant difference in the expression of *Arg1*, *Nos2*, and the ratio of *Arg1* and *Nos2* between WT and  $\Delta$ dblGATA mice (Fig. S8b,c). We next measured the mRNA levels of cytokines in the perigonadal WAT and observed a marked increase in the expression of the Th1 cytokine *Ifng* in HFD-fed  $\Delta$ dblGATA mice (Fig. 5b). In contrast, the expression levels of the Th2 cytokines *Il4* and *Il13* were significantly decreased in HFD-fed  $\Delta$ dblGATA mice (Fig. 5b).

### The cytokine expression profile in the perigonadal adipose tissue of eosinophil-deficient mice reflected defective adipocyte maturation.

To determine whether the cytokine profile in the perigonadal WAT of  $\Delta$ dblGATA mice affects adipocyte maturation, we induced the adipogenesis of 3T3-L1 cells in the presence of IFN- $\gamma$  or IL-4. As shown in Fig. 6, adipocyte-differentiated 3T3-L1 cells treated with IFN- $\gamma$  showed a significant decrease in lipid deposition as measured by Oil Red O staining. In contrast, adipocyte-differentiated 3T3-L1 cells treated with IL-4 showed an increase in lipid accumulation (Fig. 6) with significant upregulation of key adipogenic and lipogenic genes including *Cebpa*, *Acaca*, *Fasn*, and *Scd* (Fig. S9). These findings indicated that eosinophils infiltrated into the perigonadal WAT of HFD-fed mice modulate the immune microenvironment to favour adipocyte maturation.

**Eosinophil-deficient mice showed lipid accumulation in the liver.** Excessive lipid accumulation in non-adipose tissues such as the liver, muscle, and pancreas is closely associated with insulin resistance<sup>29</sup>. Given that lipids tend to be stored ectopically in the absence of functional adipocytes<sup>30</sup>, we hypothesized that eosinophil deficiency would influence the development of ectopic fat accumulation. The livers of HFD-fed  $\Delta$ dblGATA mice exhibited a paler colour and more prominent lipid deposits than those of WT mice (Fig. 7a,b). The measurement of total liver triglycerides supported the visual observation of lipid storage in the liver of HFD-fed  $\Delta$ dblGATA

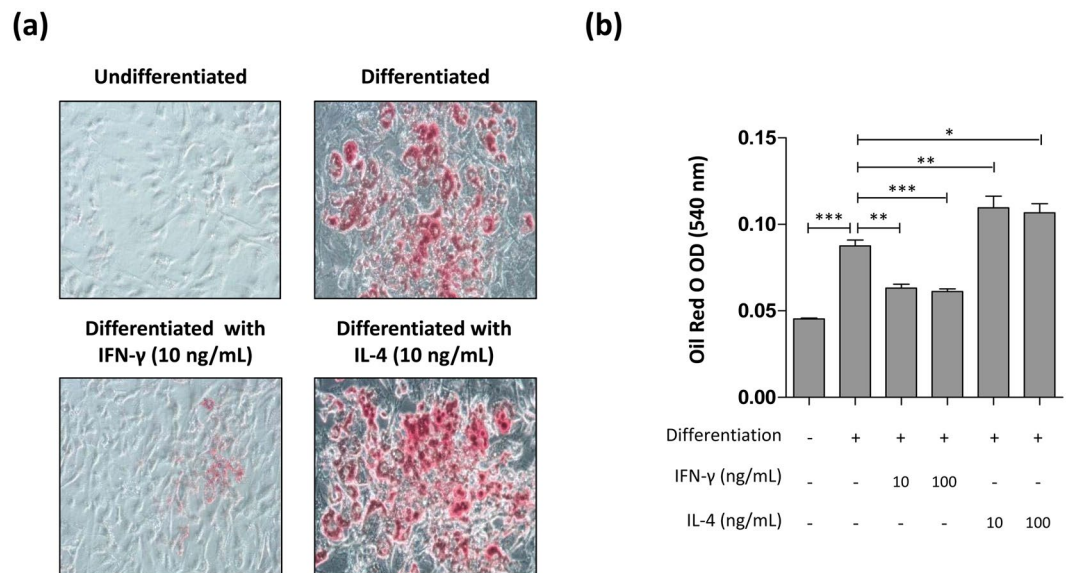


**Figure 6.** Effect of interferon (IFN)- $\gamma$  and interleukin (IL)-4 treatment on 3T3-L1 adipogenesis. **(a)** 3T3-L1 cells were treated with insulin to differentiate them into adipocytes in the presence of either IFN- $\gamma$  or IL-4 and stained with Oil Red O. Original magnification  $\times 20$ . **(b)** Oil Red O in the adipocyte-differentiated 3T3-L1 cells was eluted using isopropanol and the optical density (OD) of the eluate was analysed. \* $p < 0.05$ , \*\* $p < 0.01$ , \*\*\* $p < 0.001$  (one-way ANOVA). Graphs show the mean  $\pm$  standard error of the mean.

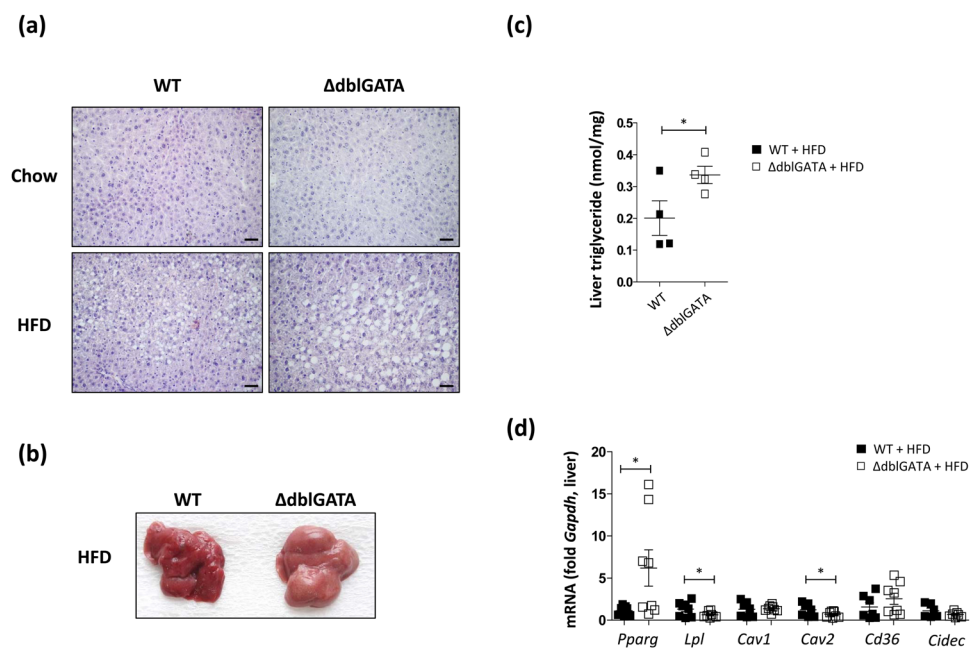


**Figure 7.** Fatty liver changes induced by high fat diet (HFD) were enhanced in  $\Delta$ dblGATA mice. **(a)** Haematoxylin and eosin staining of the liver of wild-type (WT) and  $\Delta$ dblGATA mice fed a HFD or chow diet. Images are representative of two independent experiments. Original magnification  $\times 20$ . The scale bar represents 50  $\mu$ m. **(b)** Representative image of the liver from a mouse on a HFD. **(c)** Triglyceride levels in the livers of mice fed a HFD. \* $p < 0.05$  (Student's  $t$ -test). **(d)** mRNA expression levels of adipogenic genes in the livers of mice fed a HFD. \* $p < 0.05$  (Student's  $t$ -test). Graphs show the mean  $\pm$  standard error of the mean.

mouse (Fig. 7c). An analysis of adipogenic gene expression using real-time PCR revealed a significant increase in the expression of *Pparg* in the liver of HFD-fed  $\Delta$ dblGATA mice, although the expression of *Lpl* and *Cav2* was lower in these mice (Fig. 7d). Although the lipid contents in the skeletal muscle of HFD-fed  $\Delta$ dblGATA mice was comparable to in their WT counterparts, the small intestine of HFD-fed  $\Delta$ dblGATA showed increased accumulation of triglycerides (Figs S10 and S11).

## Discussion

Although eosinophils have been characterized as destructive effector cells that mediate tissue damage during helminth infections and allergic diseases, they are found in various tissues under resting conditions without having obvious pro-inflammatory activities<sup>31,32</sup>. Accumulating evidence has indicated that tissue-resident eosinophils regulate biological processes that are not restricted to Th2 immune responses. Eosinophils in adipose tissue promote the accumulation of alternatively activated macrophages, which protect against insulin resistance induced by obesity-associated changes such as the activation of innate immune activity, alterations in fatty acid uptake, lipogenesis, and energy expenditure that can impact ectopic lipid deposition<sup>33</sup>. Obesity itself does not necessarily induce insulin resistance and primarily results from adipocytes expanding to buffer against excess nutrient uptake<sup>9</sup>. Despite recent advances in understanding the functions of eosinophils in maintaining metabolic homeostasis, their roles in adipocyte development are not fully understood. Nevertheless, multiple lines of our observation have indicated that eosinophils counteract obesity-associated metabolic dysfunctions by promoting adipocyte maturation. A significant decrease of *Ccr3* in the small intestine, lung, fat, liver, and muscle of 8–10-week-old chow diet-fed  $\Delta$ dblGATA mice imply distribution of eosinophils in the metabolic organs under resting conditions (Fig. S12). In addition, a decreased expression of genes associated with lipid metabolism was observed in the small intestine (Figs 1a and S1) and perigonadal WAT (Fig. 1c) of 8–10-week-old  $\Delta$ dblGATA mice, further suggesting that eosinophils regulate energy homeostasis. However, the expression of *Ccr3* significantly increased in the perigonadal WAT on a HFD (Fig. 4f), as well as the frequency and number of eosinophils (Figs 4h and S7a), implying the preferential infiltration of eosinophils into adipose tissue with obesity. Therefore, we propose that mature adipocytes release factors that support the infiltration of eosinophils into adipose tissue. Indeed, adipocyte-differentiated 3T3-L1 cells expressed CCL11, which has an eosinophil-selective chemoattractant activity<sup>2,3</sup>, and the CCL11 produced by 3T3-L1 cells induced the directional migration of eosinophils into adipocyte-differentiated 3T3-L1 cells (Fig. 4a–c). Adipocyte-differentiated 3T3-L1 cells also promoted the viability of eosinophils and we observed the expression of *Il3*, *Il5*, and *Csf2* (the gene encoding GM-CSF) in differentiated 3T3-L1 cells (Fig. 4d,e). These cytokines provide signals that promote the permissive proliferation and differentiation of eosinophils<sup>2,3</sup>. These findings contrast with previous observations that suggested an inverse correlation between the abundance of eosinophils in adipose tissue and adiposity<sup>5,34,35</sup>. The reasons for this difference are unclear, but mouse strains vary in their immunometabolic phenotypes<sup>36</sup>, as evidenced by the difference between BALB/c and C57BL/6 mice in their immune cell profiles with a HFD<sup>37</sup>. In line with this, chow diet-fed male C57BL/6 mice showed significantly more eosinophils in the perigonadal adipose tissue than BALB/c mice, while showing fewer eosinophils in the small intestine (Fig. S13). There are likely differences in microbiota, and thus endotoxin exposure may explain the weight difference between results of previous reports and those of our study, as exposure to microbial endotoxins may alter eosinophil maturation and activities<sup>38</sup>. Considering that our results are consistent with previous reports indicating eosinophils role in the regulation of metabolic homeostasis<sup>4,5,35</sup>, we propose that differences in mice strain and cohort might account for the divergence on eosinophil abundance in the adipose tissue between this study and previous observations.

The fat cells of adipose tissue are the only cells in the body that are designed to safely contain large amounts of fat<sup>9</sup>. Therefore, the impaired development of perigonadal adipose tissue observed in HFD-fed  $\Delta$ dblGATA mice may lead to the accumulation of lipid outside adipose tissue. The excessive accumulation of lipids in non-adipose tissues is closely associated with insulin resistance<sup>33</sup>, and we propose that ectopic fat accumulation in HFD-fed  $\Delta$ dblGATA mice might account for their glucose intolerance. Although increased visceral adiposity has been implicated in hepatic insulin resistance, patients with severe lipodystrophy, as well as a mouse model of lipodystrophy, manifest insulin resistance associated with lipid deposition in the liver<sup>39,40</sup>. The significant decrease in the expression of *Pparg*, which encodes a transcription factor involved in adipocyte differentiation, and genes associated with lipid droplet formation (*Cav1*, *Cav2*, *Cd36*, and *Cidec*) in the perigonadal WAT of HFD-fed  $\Delta$ dblGATA mice (Fig. 3) suggests insufficient lipid storage in adipose tissue in the absence of eosinophils. Concordantly, the expression of *Lpl*, *Slc2a4*, and *Adipoq*, which are regulated by *Pparg* and involved in glucose homeostasis<sup>41</sup>, significantly decreased in the perigonadal adipose tissue of HFD-fed  $\Delta$ dblGATA mice (Fig. 3). We also observed significant decreases in *Ptrf* (involved in biogenesis of caveolae), *Akt2* (involved in adipocyte differentiation and insulin signalling), and *Psm8* (involved in expression of immunogenic epitopes), which are associated with lipodystrophies, in the WAT of HFD-fed  $\Delta$ dblGATA mice (Fig. S14). We suggest that an altered immune environment in the perigonadal fat of HFD-fed  $\Delta$ dblGATA accounts for the decreased expression of adipogenic genes. The exposure of preadipocytes to pro-inflammatory cytokines inhibits adipogenesis by reducing the expression of *Pparg* and inhibiting the adipogenic action of insulin<sup>28</sup>. Th1 cytokines, including IFN- $\gamma$ , can inhibit insulin signalling and lipid droplet formation<sup>27,42</sup>, while Th2 cytokines, including IL-4 and IL-13, can suppress inflammatory responses in adipose tissue<sup>43</sup>. The increased expression of *Ifng* and decreased expression of *Il4* and *Il13* in the perigonadal fat of HFD-fed  $\Delta$ dblGATA mice imply that the microenvironments of the WAT of these mice are unfavourable for adipocyte maturation. We supported this idea by demonstrating that IFN- $\gamma$  attenuated lipid storage while IL-4 promoted lipid deposition in adipocyte-differentiated 3T3-L1 cells (Figs 6 and S9). These changes in cytokine expression were diet- and site-specific, since the expression of *Il4*, *Il13*, and *Ifng* was not different between WT and  $\Delta$ dblGATA mice either in the perigonadal adipose tissue of chow-fed mice or in the liver of HFD-fed mice (data not shown).

Obesity is associated with an increased infiltration of macrophages, preferentially the pro-inflammatory M1 phenotype, into adipose tissue<sup>22</sup>, and IL-4 produced by adipose tissue eosinophils supports the polarization of anti-inflammatory M2 macrophages<sup>5</sup>. In agreement with this idea, conditioned media (CM) collected from eosinophilic cell line EoL-1 cells or CM from palmitic-acid stimulated EoL-1 cells promoted M2-polarization of monocytic THP-1 cells (Fig. S15). However, the ratio between M1 and M2 macrophages was comparable between WT and  $\Delta$ dblGATA mice (Fig. S8), although HFD-fed  $\Delta$ dblGATA mice showed a significant decrease in the expression of *Il4* in the perigonadal WAT (Fig. 5). Given that hypoxia induces macrophage proliferation



and polarization towards the M2 phenotype<sup>44,45</sup>, it is plausible that hypoxia determined the composition of macrophages in the adipose tissue of HFD-fed  $\Delta$ dblGATA mice. The significantly elevated concentration of lactate in the perigonadal WAT of HFD-fed  $\Delta$ dblGATA mice also supports this idea (Fig. S16).

Although adipose tissue is rich in stem cells that can differentiate into fat cells to contain excess energy<sup>46</sup>, the pro-inflammatory microenvironment of adipose tissue induced by obesity is associated with the inhibition of adipocyte maturation and increased adipocyte death<sup>10,12</sup>. Our data demonstrate that adipocytes provide signals to promote eosinophil migration and survival, and that eosinophils support adipocyte maturation and protect adipose tissue against inflammatory changes. Based on our findings, we propose that eosinophils and adipocytes bidirectionally cooperate to promote metabolic homeostasis in diet-induced obesity.

## Methods

**Mice.** BALB/c WT mice (Orientbio, Gyeonggi, Korea) and  $\Delta$ dblGATA mice (C.129S1(B6)-Gata1<sup>tm6Sho/J</sup>), Jackson Laboratory, Bar Harbor, ME, USA) were housed under standard temperature and humidity in the specific pathogen-free facilities of Gachon University. Cluster of differentiation (CD) 3-IL-5 transgenic mice (NJ.1638, *IL5<sup>Tg</sup>*) were kindly provided by Dr. Jamie Lee (Mayo Clinic, Scottsdale, AZ, USA) and housed in the specific pathogen-free facilities of Tel Aviv University. Animal procedures were reviewed and approved by the Center of Animal Care and Use of Lee Gil Ya Cancer and Diabetes Institute, Gachon University (Number: LCDI-2016-0060) or by the Animal Care Committee of Tel-Aviv University (Number: M-13-029, M-13-30), and were performed in accordance with its regulations and guidelines regarding the care and use of animals for experimental procedures.

**RNA sequencing and bioinformatics analysis.** RNA isolated from the small intestine of 8–10-week-old WT ( $n = 4$ ) and  $\Delta$ dblGATA mice ( $n = 4$ ) was subjected to RNA sequencing at the Cincinnati Children's Hospital Medical Center sequencing core. Sequencing data were demultiplexed and reads were mapped to the mm10 mouse genome reference using TopHat<sup>47</sup>. The total number of mapped reads per transcript was determined and the data were normalized to detect the number of fragments per kilobase of exon per million fragments mapped (FPKM) using Cufflinks<sup>48</sup>. An FPKM  $> 0.1$  in at least 1 of the analysed samples was used to filter for potentially significant gene expression. Transcripts with fold-change values  $> 2$  with a false discovery rate-corrected  $p$ -value  $< 0.05$  were included as differentially expressed genes. Functional groups and pathways encompassing the differentially expressed genes were identified based on a Gene Ontology (GO) analysis using the Database for Annotation, Visualization, and Integrated Discovery. GO terms and pathways having an enrichment score  $> 1.3$ ,  $p$ -value  $< 0.05$ , and number of genes  $\geq 3$  were defined as significantly enriched<sup>49</sup>.

**HFD feeding and metabolic studies.** Eight-to-ten-week-old male mice were fed a HFD (60% fat, D12492, Research Diets, New Brunswick, NJ, USA) or a chow diet (5.0% fat, 5053, LabDiet, St. Louis, MO, USA) for 12 weeks. Body weight was measured weekly. Fasting insulin concentrations were measured by enzyme-linked immunosorbent assay (ELISA, Shibayagi, Gunma, Japan). For glucose tolerance tests (GTTs), glucose (1.5 g/kg) was injected intraperitoneally after starvation for 16 h and blood glucose was measured using a glucometer (Allmedicus, Kyunggi, Korea). For *in vivo* insulin signalling analysis, mice were anesthetized after overnight fasting. Insulin (0.75 U/kg) or saline was infused into the liver via the portal vein. Five minutes after infusion, liver, perigonadal fat, and skeletal muscle were quickly excised and snap-frozen in liquid nitrogen<sup>50</sup>. At sacrifice, all mice were weighed and the livers and perigonadal fat were removed and weighed.

**Total protein extraction and western blot analysis.** The tissue lysates were prepared in ice-cold tissue lysis buffer (50 mM Tris-HCl, pH 7.5; 150 mM NaCl; 1% Nonidet P-40; 0.5% sodium deoxycholate; 0.1% SDS) containing 50 mM NaF, 2 mM Na<sub>3</sub>VO<sub>4</sub>, protease inhibitors (Sigma-Aldrich, St. Louis, MO, USA) and phosphatase inhibitors (Sigma-Aldrich) and total protein was extracted as previously described<sup>50</sup>. Samples from tissue lysates were resolved by SDS-PAGE and then transferred to a nitrocellulose membrane. After 1 h blocking at 4 °C using 5% BSA in phosphate-buffered saline containing 0.1% Tween-20 (PBST), the membrane was incubated overnight with antibodies against phospho-IR $\beta$  (sc-25103, Santa Cruz Biotechnology, Santa Cruz, CA, USA), phospho-Akt (SAB5600064, Sigma-Aldrich), and  $\alpha$ -tubulin (T9026, Sigma-Aldrich) in PBST at 4 °C. After 3 PBST washes, membranes were incubated with secondary antibody for 1 h at room temperature. Chemiluminescence was performed using a SuperSignal West Pico Chemiluminescent Substrate (Thermo Fisher Scientific, Waltham, MA, USA).

**PCR analysis.** Total RNA was extracted using QIAzol<sup>®</sup> lysis reagent (Qiagen, Hilden, Germany) and subsequently column-purified with an RNeasy<sup>®</sup> Mini Kit (Qiagen). RNA (500 ng) was treated with DNase I (New England Biolabs, Ipswich, MA, USA) and cDNA was synthesized using an iScript<sup>™</sup> cDNA synthesis kit (Bio-Rad Laboratories, Hercules, CA, USA). Real-time PCR was performed using iQ SYBR<sup>®</sup> Green Supermix (Bio-Rad Laboratories) on a CFX Connect<sup>™</sup> real-time PCR detection system (Bio-Rad Laboratories). Reverse-transcription PCR was performed using Bio-ReadyMix (Bio-Lab, Jerusalem, Israel) and the amplified DNA products were electrophoresed on 2% agarose gels. The primers are detailed in Supplementary Tables S4 and S5.

**Histology.** The perigonadal fat and liver specimens were fixed in 10% buffered formalin and embedded in paraffin. Multiple 4- $\mu$ m sections were stained with haematoxylin and eosin and visualized using a CX41 microscope (Olympus, Tokyo, Japan).

**Preparation of cell suspension.** Perigonadal adipose tissues were incubated with 0.2% collagenase II (Sigma-Aldrich) in Roswell Park Memorial Institute (RPMI) 1640 medium/0.5% BSA with continuous stirring at 37 °C for 30 min. Bone marrow cells were collected by flushing the femurs with RPMI 1640 medium/5% FBS. Isolated cells were filtered through a 100- $\mu$ m cell strainer and red blood cells were lysed. For the enrichment of

leukocytes, the cells were subjected to density-gradient centrifugation in 40%/75% Percoll® (Sigma-Aldrich). The cells harvested from the interface were washed and used in subsequent assays.

**Flow cytometry.** To characterize the cell surface phenotype, isolated cells were resuspended in PBS containing 10% FCS, 20 mM HEPES, and 10 mM EDTA. After blocking Fc receptors with anti-mouse CD16/CD32 (2.4G2, BD Biosciences, San Diego, CA, USA) for 15 min at 4 °C, the cells were stained for 30 min at 4 °C with the following antibodies: mAb against CCR3 (83101) from R&D Systems (Minneapolis, MN, USA); anti-SiglecF (E50-2440) from BD Biosciences; anti-CD45 (30-F11), F4/80 (BM8), CD3 (145-2C11), and B220 (RA3-6B2) from BioLegend (San Diego, CA, USA); and anti-CD4 (RM4-5) and CD8 (53-6.7) from eBioscience (San Diego, CA, USA). Each sample was analysed with a FACSCalibur™ flow cytometer (BD Biosciences) and the data were processed using FlowJo software (Tree Star, Ashland, OR, USA).

**Isolation of eosinophils.** Eosinophils were isolated from the peritoneal cavity of CD3-IL-5 transgenic mice as described<sup>20</sup> and used for chemotaxis assay and co-culture with adipocyte-differentiated 3T3-L1 cells. Total cells were extracted and subjected to lymphocyte depletion using a MACS® system with antibodies against CD90.2 and CD45R (Miltenyi Biotec, Auburn, CA, USA). The purity and viability of the isolated cells were determined by flow cytometry and were consistently >95%.

**Adipogenesis of 3T3-L1 cells.** 3T3-L1 preadipocytes were cultured in Dulbecco's Modified Eagle's medium (DMEM) containing 10% FBS, 10 mg/mL streptomycin, and 100 U/mL penicillin at 37 °C in 5% CO<sub>2</sub>. To induce adipocyte differentiation, at 2 days post-confluence, the cells were treated with 0.5 mM isobutylmethylxanthine (Sigma-Aldrich), 10 μM dexamethasone (Sigma-Aldrich), and 1 μg/mL insulin (Sigma-Aldrich) for 72 h, followed by maintenance in DMEM containing 10% FBS and 1 μg/mL insulin. To examine the effects of cytokines on adipogenesis, the 3T3-L1 cells were treated with IFN-γ (PeproTech, Rocky Hill, NJ, USA) or IL-4 (PeproTech) during their differentiation into adipocytes.

**ELISA.** The concentrations of CCL11 (eotaxin-1) and CCL24 (eotaxin-2) secreted from adipocyte-differentiated 3T3-L1 cells were measured by ELISA according to the manufacturer's instructions (R&D Systems).

**Chemotaxis assay.** Chemotaxis was assayed using Transwell® inserts (Corning, Corning, NY, USA) with a 3-μm pore diameter. Differentiated 3T3-L1 cells were grown in DMEM containing 10% FBS at 450 μL per well until they achieved confluence. Eosinophils were loaded into each upper insert (200,000 cells in 450 μL medium). To examine the effect of chemokine blockade, anti-mouse CCL11 (PeproTech, Rehovot, Israel) was added (50 μg/mL) to the lower wells. After 24 h, the inserts were removed and the migrated cells were stained and enumerated by flow cytometry.

**Cell viability assay.** Eosinophils were cultured for 24 h with or without adipocyte-differentiated 3T3-L1 cells. Non-viability was determined by staining cells with 4',6-diamidino-2-phenylindole dihydrochloride (Sigma-Aldrich) and analysing them by flow cytometry.

**Oil Red O staining.** To evaluate lipid accumulation, adipocyte-differentiated 3T3-L1 cells were stained with Oil Red O (Sigma-Aldrich). For quantification, the dye was eluted by adding 100% isopropanol and the absorbance of the eluate was measured at 540 nm.

**Liver triglyceride quantification.** Liver triglycerides were determined with an assay kit according to the manufacturer's instructions (Biovision, Palo Alto, CA, USA).

**Statistical analysis.** Two-group comparisons were performed by Student's *t*-test or Mann-Whitney test. Data differences between groups were examined for statistical significance using two-way ANOVA with the Bonferroni post hoc test or one-way ANOVA with the Tukey post hoc test. A *p*-value < 0.05 was considered significant. The data are presented as the mean ± standard error of the mean. GraphPad Prism 5 (GraphPad, San Diego, CA, USA) was used for data analysis.

## References

- Jacobsen, E. A., Helmers, R. A., Lee, J. J. & Lee, N. A. The expanding role(s) of eosinophils in health and disease. *Blood* **120**, 3882–3890, <https://doi.org/10.1182/blood-2012-06-330845> (2012).
- Rothenberg, M. E. & Hogan, S. P. The eosinophil. *Annu. Rev. Immunol.* **24**, 147–174, <https://doi.org/10.1146/annurev.immunol.24.021605.090720> (2006).
- Jung, Y. & Rothenberg, M. E. Roles and regulation of gastrointestinal eosinophils in immunity and disease. *J Immunol* **193**, 999–1005, <https://doi.org/10.4049/jimmunol.1400413> (2014).
- Qiu, Y. *et al.* Eosinophils and type 2 cytokine signaling in macrophages orchestrate development of functional beige fat. *Cell* **157**, 1292–1308, <https://doi.org/10.1016/j.cell.2014.03.066> (2014).
- Wu, D. *et al.* Eosinophils sustain adipose alternatively activated macrophages associated with glucose homeostasis. *Science* **332**, 243–247, <https://doi.org/10.1126/science.1201475> (2011).
- Fischer, K. *et al.* Alternatively activated macrophages do not synthesize catecholamines or contribute to adipose tissue adaptive thermogenesis. *Nat. Med.* **23**, 623–630, <https://doi.org/10.1038/nm.4316> (2017).
- Pirzagska, R. M. *et al.* Sympathetic neuron-associated macrophages contribute to obesity by importing and metabolizing norepinephrine. *Nat. Med.* **23**, 1309–1318, <https://doi.org/10.1038/nm.4422> (2017).
- Hotamisligil, G. S. Inflammation and metabolic disorders. *Nature* **444**, 860–867, <https://doi.org/10.1038/nature05485> (2006).
- Sears, B. & Perry, M. The role of fatty acids in insulin resistance. *Lipids Health Dis.* **14**, 121, <https://doi.org/10.1186/s12944-015-0123-1> (2015).

10. Kim, J. Y. *et al.* Obesity-associated improvements in metabolic profile through expansion of adipose tissue. *J. Clin. Invest.* **117**, 2621–2637, <https://doi.org/10.1172/JCI31021> (2007).
11. Scherer, P. E. Adipose tissue: from lipid storage compartment to endocrine organ. *Diabetes* **55**, 1537–1545, <https://doi.org/10.2337/db06-0263> (2006).
12. Ye, J. Emerging role of adipose tissue hypoxia in obesity and insulin resistance. *Int. J. Obes. (Lond.)* **33**, 54–66, <https://doi.org/10.1038/ijo.2008.229> (2009).
13. Gregor, M. F. & Hotamisligil, G. S. Inflammatory mechanisms in obesity. *Annu. Rev. Immunol.* **29**, 415–445, <https://doi.org/10.1146/annurev-immunol-031210-101322> (2011).
14. Rosen, E. D. & Spiegelman, B. M. Adipocytes as regulators of energy balance and glucose homeostasis. *Nature* **444**, 847–853, <https://doi.org/10.1038/nature05483> (2006).
15. Chakrabarti, S. K., Cole, B. K., Wen, Y., Keller, S. R. & Nadler, J. L. 12/15-lipoxygenase products induce inflammation and impair insulin signaling in 3T3-L1 adipocytes. *Obesity (Silver Spring)* **17**, 1657–1663, <https://doi.org/10.1038/oby.2009.192> (2009).
16. Comings, D. E. *et al.* The dopamine D2 receptor (DRD2) as a major gene in obesity and height. *Biochem. Med. Metab. Biol.* **50**, 176–185 (1993).
17. Shojima, N. *et al.* Serum concentrations of resistin-like molecules beta and gamma are elevated in high-fat-fed and obese db/db mice, with increased production in the intestinal tract and bone marrow. *Diabetologia* **48**, 984–992, <https://doi.org/10.1007/s00125-005-1735-1> (2005).
18. Bindea, G. *et al.* ClueGO: a Cytoscape plug-in to decipher functionally grouped gene ontology and pathway annotation networks. *Bioinformatics* **25**, 1091–1093, <https://doi.org/10.1093/bioinformatics/btp101> (2009).
19. Gavrilova, O. *et al.* Surgical implantation of adipose tissue reverses diabetes in lipoatrophic mice. *J. Clin. Invest.* **105**, 271–278, <https://doi.org/10.1172/JCI7901> (2000).
20. Rozenberg, P. *et al.* CD300f:IL-5 cross-talk inhibits adipose tissue eosinophil homing and subsequent IL-4 production. *Sci. Rep.* **7**, 5922, <https://doi.org/10.1038/s41598-017-06397-4> (2017).
21. Mishra, A., Hogan, S. P., Lee, J. J., Foster, P. S. & Rothenberg, M. E. Fundamental signals that regulate eosinophil homing to the gastrointestinal tract. *J. Clin. Invest.* **103**, 1719–1727, <https://doi.org/10.1172/JCI6560> (1999).
22. Weisberg, S. P. *et al.* Obesity is associated with macrophage accumulation in adipose tissue. *J. Clin. Invest.* **112**, 1796–1808, <https://doi.org/10.1172/JCI19246> (2003).
23. Fabbrini, E. *et al.* Association between specific adipose tissue CD4+ T-cell populations and insulin resistance in obese individuals. *Gastroenterology* **145**, 366–374 e361-363, <https://doi.org/10.1053/j.gastro.2013.04.010> (2013).
24. Nishimura, S. *et al.* CD8+ effector T cells contribute to macrophage recruitment and adipose tissue inflammation in obesity. *Nat. Med.* **15**, 914–920, <https://doi.org/10.1038/nm.1964> (2009).
25. Winer, D. A. *et al.* B cells promote insulin resistance through modulation of T cells and production of pathogenic IgG antibodies. *Nat. Med.* **17**, 610–617, <https://doi.org/10.1038/nm.2353> (2011).
26. Elgazar-Carmon, V., Rudich, A., Hadad, N. & Levy, R. Neutrophils transiently infiltrate intra-abdominal fat early in the course of high-fat feeding. *J. Lipid Res* **49**, 1894–1903, <https://doi.org/10.1194/jlr.M800132-JLR200> (2008).
27. McGillicuddy, F. C. *et al.* Interferon gamma attenuates insulin signaling, lipid storage, and differentiation in human adipocytes via activation of the JAK/STAT pathway. *J. Biol. Chem.* **284**, 31936–31944, <https://doi.org/10.1074/jbc.M109.061655> (2009).
28. Suzawa, M. *et al.* Cytokines suppress adipogenesis and PPAR-gamma function through the TAK1/TAB1/NIK cascade. *Nat. Cell Biol.* **5**, 224–230, <https://doi.org/10.1038/ncb942> (2003).
29. Lettner, A. & Roden, M. Ectopic fat and insulin resistance. *Curr. Diab. Rep.* **8**, 185–191 (2008).
30. Unger, R. H. Lipotoxic diseases. *Annu. Rev. Med.* **53**, 319–336, <https://doi.org/10.1146/annurev.med.53.082901.104057> (2002).
31. Mesnil, C. *et al.* Lung-resident eosinophils represent a distinct regulatory eosinophil subset. *J. Clin. Invest.* **126**, 3279–3295, <https://doi.org/10.1172/JCI85664> (2016).
32. Jung, Y. *et al.* IL-1beta in eosinophil-mediated small intestinal homeostasis and IgA production. *Mucosal Immunol.* **8**, 930–942, <https://doi.org/10.1038/mi.2014.123> (2015).
33. Samuel, V. T. & Shulman, G. I. Mechanisms for insulin resistance: common threads and missing links. *Cell* **148**, 852–871, <https://doi.org/10.1016/j.cell.2012.02.017> (2012).
34. Bolus, W. R. *et al.* Elevating adipose eosinophils in obese mice to physiologically normal levels does not rescue metabolic impairments. *Mol. Metab.* **8**, 86–95, <https://doi.org/10.1016/j.molmet.2017.12.004> (2018).
35. Ding, X. *et al.* IL-33-driven ILC2/eosinophil axis in fat is induced by sympathetic tone and suppressed by obesity. *J. Endocrinol.* **231**, 35–48, <https://doi.org/10.1530/JOE-16-0229> (2016).
36. Montgomery, M. K. *et al.* Mouse strain-dependent variation in obesity and glucose homeostasis in response to high-fat feeding. *Diabetologia* **56**, 1129–1139, <https://doi.org/10.1007/s00125-013-2846-8> (2013).
37. Jovicic, N. *et al.* Differential Immunometabolic Phenotype in Th1 and Th2 Dominant Mouse Strains in Response to High-Fat Feeding. *PLoS One* **10**, e0134089, <https://doi.org/10.1371/journal.pone.0134089> (2015).
38. Buonomo, E. L. *et al.* Microbiota-Regulated IL-25 Increases Eosinophil Number to Provide Protection during Clostridium difficile Infection. *Cell Rep* **16**, 432–443, <https://doi.org/10.1016/j.celrep.2016.06.007> (2016).
39. Petersen, K. F. *et al.* Leptin reverses insulin resistance and hepatic steatosis in patients with severe lipodystrophy. *J. Clin. Invest.* **109**, 1345–1350, <https://doi.org/10.1172/JCI15001> (2002).
40. Kim, J. K., Gavrilova, O., Chen, Y., Reitman, M. L. & Shulman, G. I. Mechanism of insulin resistance in A-ZIP/F-1 fatless mice. *J. Biol. Chem.* **275**, 8456–8460 (2000).
41. Walton, R. G. *et al.* Increasing adipocyte lipoprotein lipase improves glucose metabolism in high fat diet-induced obesity. *J. Biol. Chem.* **290**, 11547–11556, <https://doi.org/10.1074/jbc.M114.628487> (2015).
42. Ranjit, S. *et al.* Regulation of fat specific protein 27 by isoproterenol and TNF-alpha to control lipolysis in murine adipocytes. *J. Lipid Res* **52**, 221–236, <https://doi.org/10.1194/jlr.M008771> (2011).
43. Ouchi, N., Parker, J. L., Lugus, J. J. & Walsh, K. Adipokines in inflammation and metabolic disease. *Nat. Rev. Immunol.* **11**, 85–97, <https://doi.org/10.1038/nri2921> (2011).
44. Murdoch, C. & Lewis, C. E. Macrophage migration and gene expression in response to tumor hypoxia. *Int. J. Cancer* **117**, 701–708, <https://doi.org/10.1002/ijc.21422> (2005).
45. Leblond, M. M. *et al.* Hypoxia induces macrophage polarization and re-education toward an M2 phenotype in U87 and U251 glioblastoma models. *Oncimmunology* **5**, e1056442, <https://doi.org/10.1080/2162402X.2015.1056442> (2016).
46. Zuk, P. A. *et al.* Human adipose tissue is a source of multipotent stem cells. *Mol. Biol. Cell* **13**, 4279–4295, <https://doi.org/10.1091/mbc.E02-02-0105> (2002).
47. Trapnell, C., Pachter, L. & Salzberg, S. L. TopHat: discovering splice junctions with RNA-Seq. *Bioinformatics* **25**, 1105–1111, <https://doi.org/10.1093/bioinformatics/btp120> (2009).
48. Trapnell, C. *et al.* Transcript assembly and quantification by RNA-Seq reveals unannotated transcripts and isoform switching during cell differentiation. *Nat. Biotechnol.* **28**, 511–515, <https://doi.org/10.1038/nbt.1621> (2010).
49. Huang da, W., Sherman, B. T. & Lempicki, R. A. Systematic and integrative analysis of large gene lists using DAVID bioinformatics resources. *Nat. Protoc.* **4**, 44–57, <https://doi.org/10.1038/nprot.2008.211> (2009).
50. Park, J. W. *et al.* Ablation of very long acyl chain sphingolipids causes hepatic insulin resistance in mice due to altered detergent-resistant membranes. *Hepatology* **57**, 525–532, <https://doi.org/10.1002/hep.26015> (2013).

## Acknowledgements

This work was supported by the Basic Science Research Program through the National Research Foundation of Korea (NRF) funded by the Ministry of Education (2016R1D1A1A09916492) and by the Center for Women In Science, Engineering and Technology (WISSET) Grant by the Ministry of Science, ICT & Future Planning of Korea (MSIP) under the Program for Returners into R&D (2017–5190). S.Y.P. and C.S.C. were supported by a grant from the Bio and Medical Technology Development Program of the NRF funded by the MSIP (2014M3A9D5A01073886) and a grant from the Korea Health Technology R&D Project through the Korea Health Industry Development Institute (KHIDI) funded by the Ministry for Health and Welfare, Korea (HI15C0987).

## Author Contributions

E.H.L. and M.I. researched data and wrote the manuscript. J.J., H.J.G., P.R., M.K.M., T.W., J.Y. and S.Y.P. researched data. J.Y.R., and C.S.C. analysed data and reviewed the manuscript. W.J.P. and A.M. analysed data, wrote and reviewed the manuscript, and contributed to discussion. Y.J. designed and supervised the studies, analysed data, and wrote and reviewed the manuscript.

## Additional Information

**Supplementary information** accompanies this paper at <https://doi.org/10.1038/s41598-018-28371-4>.

**Competing Interests:** The authors declare no competing interests.

**Publisher's note:** Springer Nature remains neutral with regard to jurisdictional claims in published maps and institutional affiliations.



**Open Access** This article is licensed under a Creative Commons Attribution 4.0 International License, which permits use, sharing, adaptation, distribution and reproduction in any medium or format, as long as you give appropriate credit to the original author(s) and the source, provide a link to the Creative Commons license, and indicate if changes were made. The images or other third party material in this article are included in the article's Creative Commons license, unless indicated otherwise in a credit line to the material. If material is not included in the article's Creative Commons license and your intended use is not permitted by statutory regulation or exceeds the permitted use, you will need to obtain permission directly from the copyright holder. To view a copy of this license, visit <http://creativecommons.org/licenses/by/4.0/>.

© The Author(s) 2018